

# Spin-Peierls transition in $\text{TiPO}_4$

J. M. Law,<sup>1,2,\*</sup> C. Hoch,<sup>1</sup> R. Glaum,<sup>3</sup> I. Heinmaa,<sup>4</sup> R. Stern,<sup>4</sup> J. Kang,<sup>5</sup> C. Lee,<sup>5</sup> M.-H. Whangbo,<sup>5</sup> and R. K. Kremer<sup>1</sup>

<sup>1</sup>Max Planck Institut für Festkörperforschung, Heisenbergstr. 1, D-70569 Stuttgart, Germany

<sup>2</sup>Physics Department, Loughborough University, Leicestershire, UK

<sup>3</sup>Institut für Anorganische Chemie, Universität Bonn, 53121 Bonn, Germany

<sup>4</sup>National Institute of Chemical Physics And Biophysics, 12618 Tallinn, Estonia

<sup>5</sup>Department of Chemistry, North Carolina State University, Raleigh, North Carolina 27695-8204, U.S.A.

(Dated: December 7, 2018)

We investigated the magnetic and structural properties of the quasi-one dimensional  $3d^1$ -quantum chain system  $\text{TiPO}_4$  ( $J \sim 965$  K) by magnetic susceptibility, heat capacity, ESR, x-ray diffraction, NMR measurements, and by density functional calculations.  $\text{TiPO}_4$  undergoes two magnetostructural phase transitions, one at 111 K and the other at 74 K. Below 74 K, NMR detects two different  $^{31}\text{P}$  signals and the magnetic susceptibility vanishes, while DFT calculations evidence a bond alternation of the Ti...Ti distances within each chain. Thus, the 74 K phase transition is a spin-Peierls transition which evolves from an incommensurate phase existing between 111 K and 74 K.

Keywords:  $\text{TiPO}_4$ , spin-Peierls, magnetic susceptibility, heat capacity, MAS NMR, DFT, ESR

The discovery of high- $T_c$  superconductivity in two-dimensional oxocuprates has stimulated broad interest in the properties of low-dimensional quantum  $S=1/2$  antiferromagnets. The complex interplay between spin, charge, orbital and lattice degrees of freedom in low-dimensional systems with pronounced quantum fluctuation renders a plethora of complex and unusual ground states.[1, 2]

Most of the prominent examples of low-dimensional quantum antiferromagnets with exotic ground states contain  $\text{Cu}^{2+}$  ( $3d^9$ ,  $S = 1/2$ ) ions with one hole present in the  $e_g$  orbitals.[3-5] Compounds of early transition-metal elements with one electron in the  $d$  shell are less frequently investigated. With a  $3d^1$  electron in a high-symmetry or slightly distorted octahedral environment, the orbital degeneracy of the  $t_{2g}$  states opens new degrees of freedom, with the possibility of low-energy orbital excitations and the interesting scenario of destabilization of coherent spin/orbital ordering by quantum fluctuations.  $3d^1$  systems can be easily realized in compounds containing, e.g.,  $\text{Ti}^{3+}$  or  $\text{V}^{4+}$  cations. A paramount example is the vanadium ladder compound  $\alpha'$ - $\text{NaV}_2\text{O}_5$ . [6] At high temperatures  $\alpha'$ - $\text{NaV}_2\text{O}_5$  contains mixed-valent vanadium cations with one electron occupying an orbital confined to the rungs of the ladder, hence constituting a quarter-filled ladder system.[7] Below  $\sim 34$  K  $\alpha'$ - $\text{NaV}_2\text{O}_5$  undergoes charge ordering[8] leading to a spin-gap of  $\sim 100$  K indicated by a rapid drop of the magnetic susceptibility. That was initially ascribed to a spin-Peierls transition.[6, 9] Other prominent low-dimensional  $3d^1$  systems that have recently attracted much attention are the Mott insulators  $\text{TiOX}$  ( $X=\text{Cl}, \text{Br}$ ). [10-14] These compounds crystallizing in the  $\text{FeOCl}$ -type structure, consisting of Ti - O - X layers made up of  $\text{TiO}_4\text{Cl}_2$  octahedra. These layers are stacked with van der Waals interactions between them.[15, 16] The magnetic susceptibility of  $\text{TiOCl}$  reveals several unusual features, which led to the proposal that  $\text{TiOCl}$  may be a manifestation of

a resonating valence-bond solid.[10] Subsequently, Seidel *et al.* demonstrated that the high temperature susceptibility fits very well to a  $S=1/2$  Heisenberg chain model with nearest-neighbor (nn) antiferromagnetic (afm) spin-exchange (SE) interaction of  $\sim 660$  K. In view of these findings and their LDA +  $U$  electronic structure calculations, Seidel *et al.* concluded that  $\text{TiOCl}$  is an example of a Heisenberg chain that undergoes a spin-Peierls transition at 67 K.[11] Subsequent low temperature x-ray structure determination showed a slight dimerization of the Ti...Ti distances along the  $b$  direction.[17] A further anomaly was detected at  $T_{c2} = 95$  K, which signals a transition into an incommensurate phase with a slight monoclinic distortion of the lattice. It was initially believed and it appears to be now generally accepted to be of continuous or higher order, however, there was a later claim that it was first order. [14, 18-21]

Here, we report the magnetic and structural properties of  $\text{TiPO}_4$ , which contains  $\text{Ti}^{3+}$  cations and displays two magneto-structural phase transitions reminiscent of those in  $\text{TiOX}$ . In contrast to  $\text{TiOCl}$ , however,  $\text{TiPO}_4$  is a structurally one-dimensional compound crystallizing in the  $\text{CrVO}_4$  structure-type (SG:  $Cmcm$ ) (see inset in Fig. 1).[22] The  $\text{Ti}^{3+}$  ions, carrying  $S=1/2$  entities, are subject to axially compressed  $\text{TiO}_6$  octahedra. These share their edges to form corrugated  $\text{TiO}_4$  ribbon chains along the  $c$ -axis with a buckling angle of  $156.927(4)^\circ$  in the  $a$ - $c$  plane. The  $\text{Ti}^{3+}\dots\text{Ti}^{3+}$  distance at room temperature (RT) amounts to  $3.1745(10)\text{\AA}$  with a  $\text{Ti}^{3+}\text{-O}^{2-}\text{-Ti}^{3+}$   $\angle$  of  $95.484(5)^\circ$ . [23] The  $\text{TiO}_4$  ribbon chains are interconnected by sharing corners with distorted  $\text{PO}_4$  tetrahedra.

At high temperature the magnetic susceptibility of a polycrystalline sample (Fig. 1, main panel) is characterized by a broad maximum centered at  $\sim 625$  K, indicating short range afm correlations. After correction for a temperature independent offset to the susceptibility arising from diamagnetic contributions of the closed shells and van Vleck terms, the high temperature magnetic suscep-

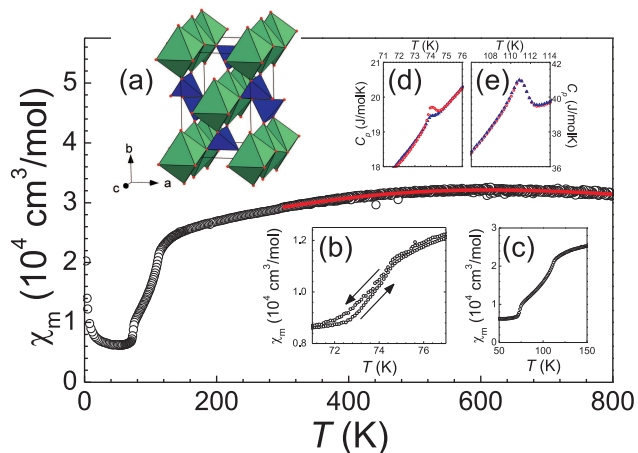


FIG. 1: (Color online) (a) Crystal structure of  $\text{TiPO}_4$ , where green and blue polyhedral represent the  $\text{TiO}_6$  octahedra and  $\text{PO}_4$  tetrahedra, respectively. (b, c)  $\chi_m$  in the region of the phase transitions. (d, e) Heat capacity,  $C_p$ , in the region of the anomalies, where the red circles and blue triangles refer to the heating and cooling data, respectively.

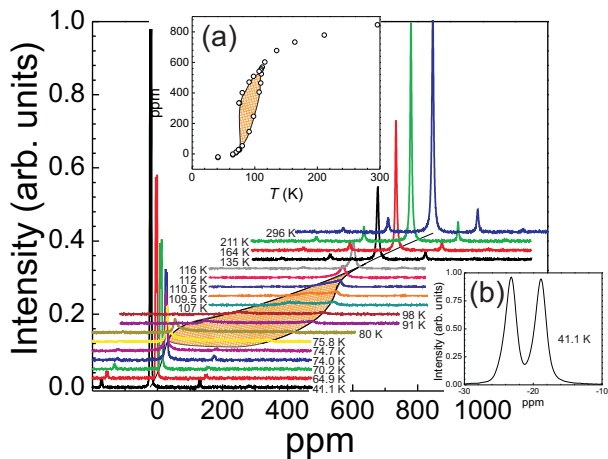


FIG. 2: (Color online)  $^{31}\text{P}$  MAS NMR spectra for  $\text{TiPO}_4$  (temperatures indicated). The (orange) hashed area highlights the incommensurate continuum. Insets: (a) Peak positions and/or boundary edges versus temperature. (b) The 41.1 K spectrum.

tibility can be described very well by a  $S=1/2$  Heisenberg chain with a uniform nn afm SE interaction[24] of  $965(10)$  K and a  $g$ -factor of  $1.94(3)$ .

Below  $\sim 120$  K the susceptibility reveals two subsequent magnetic phase transitions, indicated by two rapid drops of the susceptibility at  $111(1)$  K and  $74(0.5)$  K. Finally, at lowest temperatures the susceptibility levels off to a value of  $75(10) \times 10^{-6} \text{ cm}^3/\text{mol}$ . At very low tem-

perature a slight increase is seen, which we ascribe to a Curie tail due to  $\sim 70$  ppm of a free  $S=1/2$  spin entities. The anomaly at 74 K shows a thermal hysteresis with a temperature difference of  $\sim 50$  mK between the heating and cooling traces while heating/cooling cycles gave identical susceptibilities for the 111 K anomaly (see Fig. 1 inset (b, c)).

Heat capacities collected on crystals exhibit two  $\lambda$ -type anomalies at  $110.9(0.6)$  K and  $74.1(0.3)$  K, with the lower temperature anomaly also showing a thermal hysteresis, while again no hysteresis is seen for the higher temperature anomaly (see Fig. 1 inset (d, e)). Angular and temperature dependent Electron Spin Resonance measurements (ESR) on single crystals revealed a single Lorentzian resonance line ( $g$ -factor 1.93 - 1.95) and a linewidth decreasing linearly with temperature ( $50 \text{ Oe} \leq \text{FWHM} \leq 300 \text{ Oe}$ ) consistent with earlier findings.[22, 25] The integrated intensity of the ESR line mimics the temperature dependence of the magnetic susceptibility and drops to zero below 74 K.

The crystal structure of a very high quality single crystal of  $\text{TiPO}_4$  was determined by x-ray single crystal diffraction measurements at various temperatures between 293 K and 90 K. Down to 90 K the structure was found to be identical to that reported by Glaum *et al.*, except for small changes of the lattice parameters and the general atomic positions.[23] As the temperature is lowered from RT to  $\sim 120$  K, the lattice parameters  $a$  and  $b$  increase slightly but the  $c$  parameter decreases, such that the cell volume remains almost constant. The residual electron density, i.e. the measured electron density minus the calculated electron density (from the superposition of spherical atom densities) shows considerable residuals located within the  $a$  -  $c$  plane next to the Ti atoms, at an interstitial position in the ribbon chain, and at a position bisecting the O - Ti - O angle perpendicular to the ribbon chains. Upon cooling there is a gradual migration of the density away from the bisecting position into the interstitial position within the ribbon chains. This change is complemented by a reduction of the distance in the Ti - O - Ti, nn super-exchange pathway, and an increase of the intrachain O - Ti - O angle. Evidence for a structural change was not found in this temperature range, possibly due to the dynamic character of the intermediate phase as observed by NMR (see below).

Magic angle spinning (MAS)  $^{31}\text{P}$  nuclear magnetic resonance (NMR) spectra (center field  $\sim 8.5$  T) operating at a spinning frequency of  $\sim 25$  kHz, were collected on a polycrystalline sample between  $\sim 35$  K and RT. The spectra are displayed versus temperature in the main panel of Fig. 2. Above  $\sim 140$  K we observe a single  $^{31}\text{P}$  symmetric NMR line accompanied by two sets of very weak symmetrically placed spinning sidebands. Near 116 K the line becomes asymmetric and below 111 K it broadens into an asymmetric continuum limited by two boundary peaks. With decreasing temperature the

continuum expands and its intensity decreases. Towards  $\sim 76$  K the continuum finally washes out, whereupon its lower boundary grows into two symmetric lines indicating the occurrence of two different P atom environments (see inset Fig. 2 (b)). The peak positions and/or boundary edges are shown versus temperature in Fig. 2 (a). There are similarities between NMR measurements of  $\text{TiPO}_4$ , reported here, and  $\text{TiOX}$ , reported by Saha *et al.*[26]

We now probe the SE interactions of  $\text{TiPO}_4$  by performing mapping analysis based on density functional calculations.[27] We consider the nn and next-nearest neighbor (nnn) intrachain SE interactions  $J_1$  and  $J_2$ , respectively, as well as the interchain SE interaction  $J_3$  (see Fig. 3). To evaluate  $J_1 - J_3$ , we determine the relative energies of the four ordered spin states, FM, AF1, AF2, and AF3 shown in Fig. 3, by density functional theory (DFT) electronic band structure calculations. Our DFT calculations employed the Vienna *ab initio* simulation package (Ref. 28, 29) with the projected augmented-wave method, the generalized gradient approximation (GGA) for the exchange and the correlation functional.[30] We used a plane-wave cut-off energy of 400 eV, a set of 56  $\mathbf{k}$ -point irreducible Brillouin zone, and the threshold of  $10^{-5}$  eV for the self-consistent-field convergence of the total electronic energy. To account for the electron correlation associated to the Ti  $3d$  state, we performed GGA plus onsite repulsion (GGA+ $U$ ) calculations (Ref. 31) with an effective  $U_{\text{eff}} = U - J = 2$  eV and 3 eV on Ti. The relative energies, per four formula units (FUs), of the four ordered spin states are summarized in Fig. 3.

The total SE energies of the four ordered spin states can be expressed in terms of a Heisenberg spin Hamiltonian,  $H = -\sum J_{ij} \vec{S}_i \cdot \vec{S}_j$ , where  $J_{ij}$  is the SE interaction between the spins  $\vec{S}_i$  and  $\vec{S}_j$  on the spin sites  $i$  and  $j$ , respectively. By applying the energy expressions obtained for spin dimers with  $N$  unpaired spins per spin site (in the present case,  $N = 1$ ),[32], the total SE energies for the four configurations, per four FUs, are given in Fig. 3.

Thus, by mapping the relative energies of the four ordered spin configurations given in terms of the SE parameters (see Fig. 3) onto the corresponding relative energies obtained from the GGA+ $U$  calculations, we obtained the values for the SE parameters  $J_1 - J_3$  (see Table I).[27, 33] The results of our DFT calculations are in very good quantitative agreement with our experimental findings indicating a very large nn intrachain afm SE interaction. The nnn intrachain SE interaction is almost two orders of magnitude smaller, the interchain interaction  $J_3$  amounts to 2% of  $J_1$ .

The low temperature MAS data of  $\text{TiPO}_4$  prove a non-magnetic ground state with two distinct P atomic environments, as evidenced especially by the low temperature spectra. The chemical shifts of the  $^{31}\text{P}$  lines amount to  $\sim -20$  ppm in good agreement with what has been found for other diamagnetic orthophosphates,

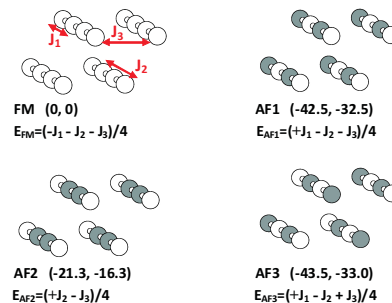


FIG. 3: (Color online) The four ordered spin configurations, FM, AF1, AF2 and AF3, used to extract the values of  $J_1$ ,  $J_2$  and  $J_3$ , where only the  $\text{Ti}^{3+}$  ions are shown for simplicity. The up- and down-spin  $\text{Ti}^{3+}$  sites are indicated by different colors. The numbers in parenthesis (from left to right) represent the relative energies in meV per four FUs obtained from GGA+ $U$  calculations with  $U_{\text{eff}} = 2$  and 3 eV, respectively. The expression of the total SE energy per four FUs is also given.

$J_i$	$U = 2\text{eV}$	$U = 3\text{eV}$
$J_1$	-988	-751
$J_2$	-1.4	+0.7
$J_3$	-20	-15

TABLE I: Values of the SE parameters  $J_1 - J_3$  derived from the mapping analysis (in K).

proving the non-magnetic character of the ground state of  $\text{TiPO}_4$ . [34, 35] We ascribe the 74 K phase transition in  $\text{TiPO}_4$  to a spin-Peierls transition with the Ti...Ti bond alternation within the Ti chains.

To probe the low temperature crystal structure of  $\text{TiPO}_4$ , we considered the subgroups  $Amm2$  and  $Pmnm$  of the RT space group  $Cmcm$ . By GGA calculations, we optimized the structures of  $\text{TiPO}_4$  starting with the initial settings described by  $Cmcm$ ,  $Amm2$  and  $Pmnm$  without symmetry constraints in order to allow the atom positions to relax freely (with a set of 28  $\mathbf{k}$ -point irreducible Brillouin zone, and the thresholds of  $10^{-5}$  eV and 0.001 eV/Å for the self-consistent-field convergence of the total electronic energy and force, respectively). The lowest-energy structure found was obtained starting from the  $Pmnm$  initial setting, and was lower in energy by  $\sim 48$  meV per formula unit than was the  $Cmcm$  structure, and by  $\sim 32$  meV per formula unit than the  $Amm2$  initial structure. The structure relaxed from the  $Pmnm$  initial setting shows a dimerization in the Ti chains with alternating Ti...Ti distances of  $\sim 2.9$  and  $\sim 3.5$  Å, which is comparable in magnitude to that

observed in TiOCl.[17] This structure also has two different environments for the P atoms within the PO<sub>4</sub> units, which is consistent with our MAS NMR spectra. From model calculations using the relaxed crystal structure data, we expect very weak superstructure reflections, which were not resolved in an early neutron powder diffraction experiment.[36]

The incommensurate phase seen between  $\sim 111$  K and  $\sim 74$  K is similar to that found for TiOX, where it has been attributed to a frustration between the spin-Peierls pairing and an elastic interchain coupling.[20] Analogous arguments may apply for TiPO<sub>4</sub> as well. In view of the small interchain coupling the incommensurate phase between 111 K and 74 K could also be ascribed to a dynamic equilibrium between short-range-ordered dimerized segments.

In conclusion, our magnetic susceptibility, heat capacity, ESR and <sup>31</sup>P MAS NMR measurements supported by our density functional calculations show that TiPO<sub>4</sub> undergoes a spin-Peierls transition at 74.1(0.3) K, which is preceded by an incommensurate phase extending up to  $\sim 111$  K. The thermal hysteretic behavior of these transitions is consistent with the pattern of discontinuous and continuous transitions seen for TiOCl and TiOBr. At high temperatures the magnetic susceptibility of TiPO<sub>4</sub> is described by a  $S=1/2$  Heisenberg antiferromagnetic chain with an unprecedented nn SE of  $\sim 1000$  K.

Work at NCSU by the Office of Basic Energy Sciences, Division of Materials Sciences, U. S. Department of Energy, under Grant DE-FG02-86ER45259, and also by the computing resources of the NERSC center and the HPC center of NCSU.

---

\* Electronic address: j.law@fkf.mpg.de

- [1] E. Dagotto, *Science* **309**, 257 (2005).
- [2] P. A. Lee, *Rept. Prog. Phys.* **71**, 012501 (2008).
- [3] M. Enderle, C. Mukherjee, B. Fåk, R. K. Kremer, J.-M. Broto, H. Rosner, S.-L. Drechsler, J. Richter, J. Malek, A. Prokofiev, W. Assmus, S. Pujol, J.-L. Raggazzoni, H. Rakoto, M. Rheinstädter, and H. M. Rønnow, *Europhys. Lett.* **70**, 237 (2005).
- [4] M. G. Banks, R. K. Kremer, C. Hoch, A. Simon, B. Ouladdiaf, J. M. Broto, H. Rakoto, C. Lee, and M.-H. Whangbo *Phys. Rev. B*, **80**, 024404 (2009).
- [5] J. M. Law, C. Hoch, M.-H. Whangbo, and R. K. Kremer, *Z. anorg. allg. Chem.*, **636**, 54 (2010).
- [6] M. Isobe and Y. Ueda, *J. Phys. Soc. Jpn.* **65**, 1178 (1996).
- [7] H. Smolinski, C. Gros, W. Weber, U. Peuchert, G. Roth, M. Weiden, and Ch. Geibel, *Phys. Rev. Lett.* **80**, 5164 (1998).
- [8] J. Lüdecke, A. Jobst, S. van Smaalen, E. Morr e, Ch. Geibel, and H.-G. Krane, *Phys. Rev. Lett.* **82**, 3633 (1999).
- [9] M. Weiden, R. Hauptmann, C. Geibel, F. Steglich, M. Fischer, P. Lemmens, and G. Guntherodt, *Z. Phys. B* **103**, 1 (1997).
- [10] R. J. Beynon and J. A. Wilson, *J. Phys.: Condens. Matter* **5**, 1983 (1993).
- [11] A. Seidel, C. A. Marianetti, F. C. Chou, G. Ceder, and P. A. Lee, *Phys. Rev. B* **67**, 020405 (2003).
- [12] V. Kataev, J. Baier, A. Moller, L. Jongen, G. Meyer, and A. Freimuth, *Phys. Rev. B* **68**, 140405 (2003).
- [13] R. Ruckamp, J. Baier, M. Kriener, M. W. Haverkort, T. Lorenz, G. S. Uhrig, L. Jongen, A. M ller, G Meyer, and M. Gr ninger, *Phys. Rev. Lett.* **95**, 097203 (2005).
- [14] A. Krimmel, J. Stremper, B. Bohnenbuck, B. Keimer, M. Hoinkis, M. Klemm, S. Horn, A. Loidl, M. Sing, R. Claessen, and M. v.Zimmermann, *Phys. Rev. B* **73**, 172413 (2006).
- [15] H. Sch fer, F. Wartenpfehl, and E. Weise, *Z. Anorg. Allg. Chem.* **295**, 268 (1958).
- [16] H. G. von Schnering, M. Collin, and M. Hassheider, *Z. Anorg. Allg. Chem.* **387**, 137 (1972).
- [17] M. Shaz, S. van Smaalen, L. Palatinus, M. Hoinkis, M. Klemm, S. Horn, and R. Claessen, *Phys. Rev. B* **71**, 100405(R) (2005).
- [18] Y.-Z. Zhang, H. O. Jeschke, and R. Valent , *Phys. Rev. B* **78**, 205104 (2008).
- [19] J. Hemberger, M. Hoinkis, M. Klemm, M. Sing, R. Claessen, S. Horn, and A. Loidl, *Phys. Rev. B* **72**, 012420 (2005).
- [20] A. Sch nleber, G. Shcheka, and S. van Smaalen, *Phys. Rev. B* **77**, 094117 (2008).
- [21] J. P. Clancy, B. D. Gaulin, and F. C. Chou, *Phys. Rev. B* **81**, 024411 (2010).
- [22] N. Kinomura and F. Muto, *J. Solid State Chem.*, **46**, 252 (1982).
- [23] R. Glaum and R. Gruehn, *Z. Kristallogr.*, **198**, 41 (1992).
- [24] D. C. Johnston, R. K. Kremer, M. Troyer, X. Wang, A. Kl mper, S. L. Budko, A. F. Panchula, and P. C. Canfield, *Phys. Rev. B* **61**, 9558 (2000).
- [25] R. Glaum and M. A. Hitchman, *Australian J. Chem.*, **49**, 1221 (1996).
- [26] S. R. Saha, S. Golin, T. Imai, and F.C. Chou, *J. Phys. Chem. Solids* **68**, 2044 (2007).
- [27] M.-H. Whangbo, H.J. Koo, and D. J. Dai, *Solid State Chem.* **176**, 417 (2003).
- [28] G. Kresse and J. Hafner, *Phys. Rev. B* **47**, 558 (1993).
- [29] G. Kresse and J. Furthm ller, *Comput. Mater. Sci.* **6**, 15 (1996); G. Kresse and J. Furthm ller, *Phys. Rev. B* **54**, 11169 (1996).
- [30] J. P. Perdew, K. Burke, and M. Ernzerhof, *Phys. Rev. Lett.* **77**, 3865 (1996).
- [31] S. L. Dudarev, G. A. Botton, S. Y. Savrasov, C. J. Humphreys, and A. P. Sutton, *Phys. Rev. B* **57** 1505 (1998).
- [32] D. Dai, and M.-H. Whangbo, *J. Chem. Phys.* **114**, 2887 (2001); D. Dai, and M.-H. Whangbo, *J. Chem. Phys.* **118**, 29 (2003).
- [33] H.-J. Koo, M.-H. Whangbo, and K.-S. Lee, *Inorg. Chem.*, **42**, 5932 (2003).
- [34] A. K. Cheetham, N. J. Clayden, C. M. Dobson, and R. J. B. Jakemana *J. Chem. Soc., Chem. Commun.*, p. 195 (1986).
- [35] G. L. Turner, K. A. Smith, R. J. Kirkpatrick, and E. Oldfield, *J. Mag. Res.* **67**, 544 (1986).
- [36] R. Glaum, M Reehuis, N. St i er, U. Kaiser, and F. Reinauer, *J. Solid State Chem.*, **126**, 15 (1996).